JOURNAL OF SYNCHROTRON RADIATION

ISSN 1600-5775

Received 4 April 2019
Accepted 25 April 2019

Edited by P. A. Pianetta, SLAC National Accelerator Laboratory, USA

**Keywords:** compound refractive lenses; X-ray microscopy; synchrotron radiation.

**Supporting information**: this article has supporting information at journals.iucr.org/s

# CRL-based ultra-compact transfocator for X-ray focusing and microscopy

**Anton Narikovich,[a] Maxim Polikarpov,[b] Alexander Barannikov,[a] Nataliya Klimova,[a] Anatoly Lushnikov,[a] Ivan Lyatun,[a] Gleb Bourenkov,[b] Dmitrii Zverev,[a] Igor Panormov,[a] Alexander Sinitsyn,[a] Irina Snigireva[c] and Anatoly Snigirev[a]***

[a]Immauel Kant Baltic Federal University, Nevskogo 14, 236041 Kaliningrad, Russian Federation, [b]European Molecular Biology Laboratory, Hamburg Unit, Notkestraße 85, 25a, 22607 Hamburg, Germany, and [c]European Synchrotron Radiation Facility, BP 220, 38043 Grenoble, France. *Correspondence e-mail: asnigirev@kantiana.ru

A new ultra-compact transfocator (UCTF) based on X-ray compound refractive lenses (CRLs) is presented. The device can be used to change the number of one- and two-dimensional focusing CRLs by moving the individual parabolic lenses one-by-one independently, thus providing permanent energy and focal-length tunability for scanning and full-field X-ray microscopy applications. The small overall size and light weight of the device allow it to be integrated in any synchrotron beamline, while even simplifying the experimental layout. The UCTF was tested at the Excillium MetalJet microfocus X-ray source and at the P14 EMBL (PETRA-III) beamline, demonstrating high mechanical stability and lens positioning repeatability.

## 1. Introduction

Since the first successful implementation of X-ray compound refractive lenses (CRLs) (Snigirev *et al.*, 1996), they have become standard elements at many synchrotron beamlines (Dimper *et al.*, 2014). Modifying shape, composition and number of individual lenses, CRLs can be adapted to photon energies from 2 keV to 200 keV, providing flexible adjustment of focal lengths and versatility for a wide range of applications (Snigirev & Snigireva, 2008). CRLs can provide beam conditioning functions, *i.e.* condensers (Polikarpov, Snigireva and Snigirev, 2016), collimators (Baron *et al.*, 1999; Chumakov *et al.*, 2000), beam-shapers (Zverev *et al.*, 2017) and higher-harmonic suppressors (Polikarpov *et al.*, 2014). Currently, CRLs are extensively used in X-ray imaging and microscopy (Byelov *et al.*, 2013; Zverev *et al.*, 2017, 2018), interferometry (Snigirev, Snigireva, Kohn *et al.*, 2009; Snigirev *et al.*, 2014; Zverev *et al.*, 2018) and spectroscopy (Santoro *et al.*, 2014). Use of refractive optics allows us to track dynamical and structural transformations, which is especially important in studies of materials under extreme conditions (Dubrovinskaia *et al.*, 2016) and in high-resolution X-ray diffraction experiments (Drakopoulos *et al.*, 2005; Ershov *et al.*, 2015).

In a typical X-ray experiment, a considerable number of individual lenses have to be coaxially grouped to focus radiation at a certain distance and given energy. A system with arrays of planar refractive lenses aligned in parallel was designed to combine the advantages of compound refractive optics with the precise alignment possibilities of planar microfabrication technologies (Snigirev *et al.*, 2002, 2007; Polikarpov, Polikarpov *et al.*, 2016). To align two-dimensional lenses in experiments with tunable energies, however, a system

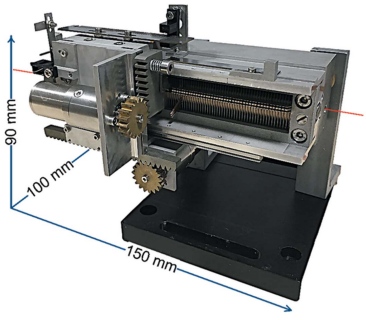

with a variable number of lenses in the stack, a so-called transfocator (TF), was proposed (Snigirev, Snigireva, Vaughan *et al.*, 2009). The first in-vacuum white-beam TF was installed at the ID11 beamline at the ESRF and demonstrated long-term stability during the years of micro-focusing operation (Vaughan *et al.*, 2011). The simplicity and versatility of TFs has led to their widespread use (Zozulya *et al.*, 2012), changing the concept of synchrotron beamlines (Bowler *et al.*, 2015; Snigirev *et al.*, 2018). Transfocators have been used to optimize beam size and divergence in a great range of experimental techniques such as high-resolution transmission X-ray microscopy for mesoscopic materials (Bosak *et al.*, 2010), time-resolved X-ray scattering (Buffet *et al.*, 2012) or resonant and non-resonant elastic scattering and diffraction (Strempfer *et al.*, 2013).

Despite all the benefits, up to now all in-vacuum or in-air TFs have the disadvantage of large size, which limits their usage as short-focal magnifying objectives. For instance, this is an issue for dark-field X-ray microscopy (Simons *et al.*, 2015), where a TF should be set less than 10 cm from the sample. The large size is mainly caused by the fact that TFs contain cartridges with lenses grouped by powers of two. This layout leaves gaps between some lenses, which is exacerbated by further enlargement due to the need for cooling or vacuum systems. Here, we propose a new technological solution: an ultra-compact transfocator (UCTF) with special holders that provide precise and close positioning of individual lenses. In the following sections, we will describe technical characteristics of the device and demonstrate its optical performance at both laboratory and synchrotron X-ray sources.

## 2. The design

The UCTF [Fig. 1(*a*)] has been designed and manufactured at the International Research Center 'Coherent X-ray Optics for Megascience Facilities', Immanuel Kant Baltic Federal University (IKBFU), Russia. The main distinctive feature of the device is a single-lens approach, which means that individual parabolic lenses are moving one-by-one independently. The UCTF contains 50 individual X-ray refractive lenses located in special holders called lamellae [Fig. 1(*b*)] with a thickness of 1 mm. Copper lamellae are separated by thin spacers (0.4 mm thick) to prevent them from rubbing against each other while moving. In contrast to the cartridge design of existing TFs, our layout minimizes the distance between individual lenses, which reduces possible misalignments and aberrations.

By default, all lamellae touch the bottom surface of the UCTF due to gravity, and all lenses are inserted in the photon beam. After which, lenses can be taken out of the beam, moving the lamellae driver vertically by two actuators – the first one slides along the beam optical axis to select the desirable number of lamellae while the second one pushes this amount in and out of the photon beam [see Fig. 1(*c*), and Video S1 in the supporting information]. Therefore, the number of inserted lenses can vary progressively with a step of one, providing smooth variation of foci and predictable focal positions.

Using the single-lens approach, we made the UCTF more compact with a length, width and height of 150 mm, 100 mm and 90 mm, respectively. All parts of the device were mounted

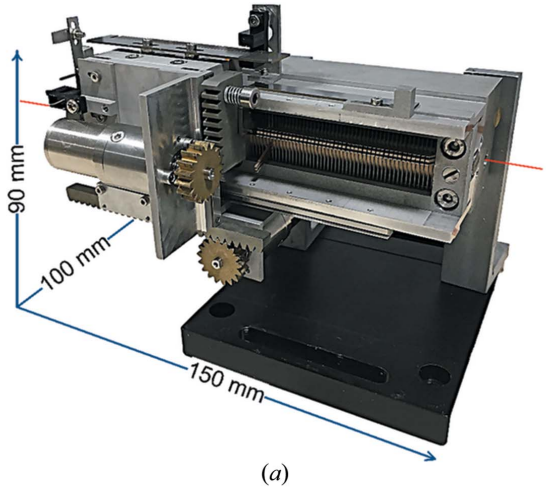


(*a*)


(*b*)

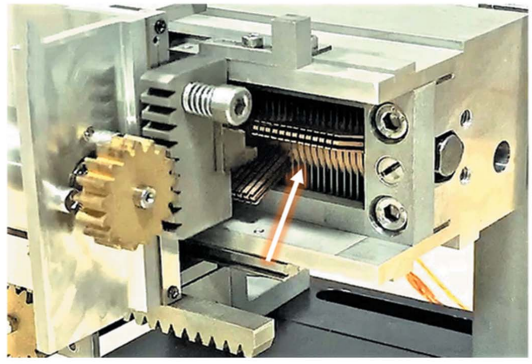

(*c*)


(*d*)

**Figure 1**
(*a*) X-ray UCTF has the minimal dimensions that are on the limit of the size of individual lamellae (*b*). (*c*) The arrow points at 13 lamellae in the beam path while all others are retracted from the beam with the lamella driver. (*d*) Photograph of the control unit.

on a single-wireframe unit, which allowed us to reduce the weight of the device to less than 2 kg.

The UCTF has a control unit [Fig. 1(*d*)] based on the single-board RaspberryPi (Raspberry Pi Foundation, https://www.raspberrypi.org/about/) computer with Raspbian 4.9 OS. A special Python-based software was designed to provide high-level access to device-control functions with the possibility to create custom commands. The software can be integrated into most modern synchrotron beamline controlling systems such as SPEC or ACTL.

## 3. Experimental tests

First, the UCTF was tested for mechanical performance and positioning repeatability at the Micro-optics test bench (MOTB) at IKBFU. For the test, we inserted 20 parabolic two-dimensional lenses [Fig. 2(*a*)] inside the UCTF. Lenses were manufactured at the International Research Center 'Coherent X-ray Optics for Megascience Facilities' (IKBFU) from polycrystalline aluminium by a pressing technique. Each lens had a geometric aperture of 0.5 mm and a 50 µm radius of curvature. Lenses were grouped in four stacks with five lenses each, and the stacks were separated by ten empty lamellae.

MOTB comprises the Excillum MetalJet D2 X-ray source (Excillum AB, Torshamnsgatan, Kista, Sweden; https://www.excillum.com/) which produces X-ray radiation of 9.25 keV (Ga $K\alpha$ line) within the source area of 15 µm × 15 µm. The UCTF was mounted at a distance of 2 m from the X-ray source on a motorized stage with five degrees of freedom (vertical and horizontal translations, roll, pitch and yaw) with angular motor resolutions of 0.01°. At a distance of 13 cm behind the UCTF, we placed the photon-counting detector Timepix STPX-65k (Amsterdam Scientific Instruments). The goal of the test was to measure the positioning accuracy of lamellae by inserting different sets of lenses and measuring the deviation of the optical axis. The position of the optical axis was defined with angular motors, by adjustment to the maximum intensity transmitted through the UCTF and measured with the ASI detector.

In the first part of the test, we repeatedly inserted and retracted all 50 lamellae. In this case, the geometric center of the resulting compound refractive lens ($CRL_{20}$) – the point which is equidistant from the beginning and the end of the $CRL_{20}$ – coincided with the center of mass of the UCTF. As a result, we found that the optical axis did not deviate by more than 0.01° from one measurement to another. This number also corresponded to the accuracy of the motorized angular stage so it limited the precision of our measurements.

In the next part, we inserted $CRL_{20}$ into the beam path. Then, we repeatedly retracted 10 lenses (20 lamellae in a row) and reinserted them, measuring the displacement of the optical axis between these two conditions. Note that the geometric center of the compound refractive lens with 10 single lenses ($CRL_{10}$) was shifted relative to the center of the $CRL_{20}$ (with 20 lenses) by 12 mm. It meant that this test was more sensitive to possible positioning misalignments of individual lamellae. As a result, the optical axis was shifted by 0.03° after switching from one CRL to another, indicating that individual lamellae were not evenly pressed by the lamella driver along the optical axis. Therefore, we manufactured new lamellae from a beryllium–copper alloy. Compared with the previously used copper-based alloy, it had greater strength, elastic limit and relaxation resistance, higher electrical and thermal conductivity, and resistance to corrosion and corrosion fatigue. In addition, lamellae were manufactured in the framework of a single technological process to improve the similarity.

To improve measurement accuracy, further tests were made at the P14 EMBL beamline of PETRA-III (c/o DESY). P14 uses a standard U29 undulator (Barthelmess *et al.*, 2008) with an effective source size of approximately 30 µm × 350 µm full width at half-maximum (FWHM) in the vertical and horizontal directions, respectively. Employing a liquid-nitrogen-cooled vertical-offset double-crystal Si(111) monochromator, an energy of 12.7 keV was selected for the experiment. The UCTF was mounted on the translation stage located at $L_1$ = 68 m from the source [Fig. 2(*b*)]. The stage offered five degrees of freedom (vertical and horizontal translation, roll, pitch and yaw) with linear motor resolutions of 5 µm.

For this part of the test, we used beryllium parabolic refractive two-dimensional lenses. A total of 17 single lenses of two types were alternately placed inside the UCTF: $N$ = 8 lenses with a 500 µm radius of curvature and $N$ = 9 lenses with a 200 µm radius of curvature. The aperture of the lenses was limited by an 800 µm upstream pinhole. We will call this arrangement $CRL_{17}$. $CRL_{17}$ had a focal distance of $F$ = 3.9 m for the selected photon energy. Therefore, according to the thin-lens formula, $1/F = 1/L_1 + 1/L_2$, the UCTF focused the incoming radiation at an imaging distance of $L_2$ = 4.1 m downstream, producing a demagnified image of the undulator source. The image was recorded using an X-ray imaging system consisting of a thin (2.6 µm) GGG:Eu scintillator

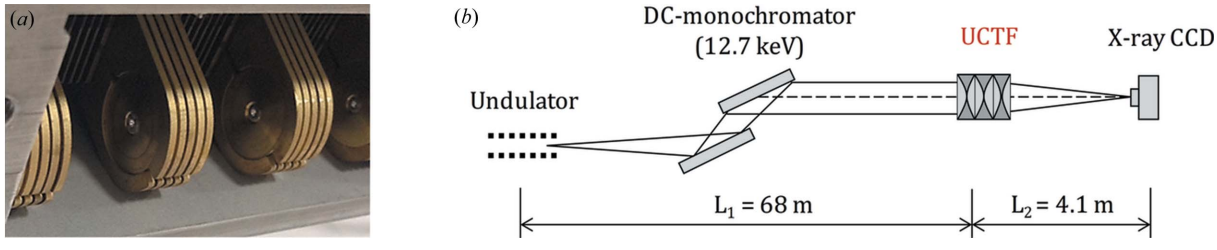


**Figure 2**
(*a*) Photograph of the arrangement of the lamellae for the laboratory test. (*b*) Layout of the experiment at the P14 beamline.

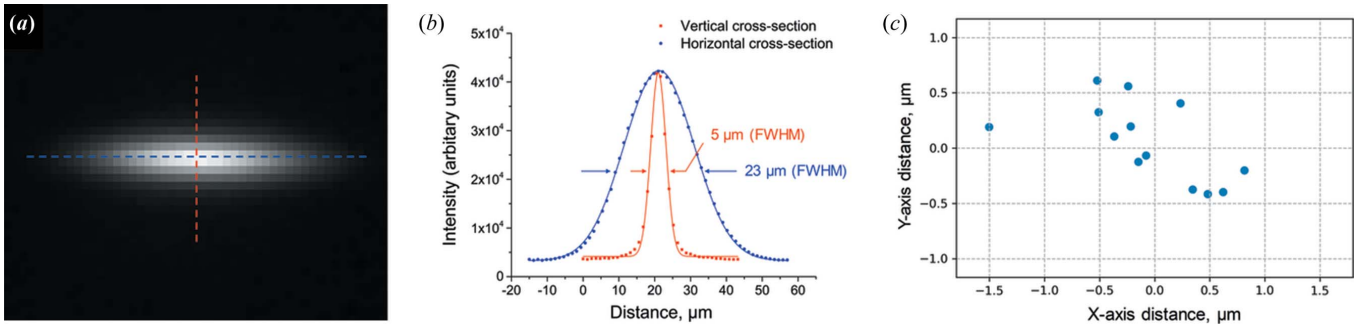


**Figure 3**
(*a*) Image of the X-ray source with (*b*) vertical and horizontal cross-sections and (*c*) the stability test results.

(CEA-Leti, Grenoble, France), a 45° mirror reflection of the image of the scintillator upwards, an OLYMPUS UPlanFI tenfold objective (OLYMPUS, Tokyo, Japan) and a DALSA Pantera TF 1M60 CCD-camera (Teledyne, Waterloo, Canada) with 1024 pixels × 1024 pixels and a 1–58 frames $s^{-1}$ acquisition frequency. Taking into account all optical elements, the imaging setup resulted in an effective pixel size of 1.2 μm. As seen from Fig. 3, the obtained focal spot was 5 μm × 23 μm (FWHM of the intensity distribution) in the vertical and horizontal directions, respectively. The main purpose of the test was to check lens positioning repeatability, so we inserted and retracted $CRL_{17}$ 15 times, recording the positions of the focal spot. The X-ray camera acquired 50 images at 25 frames $s^{-1}$ for every positioning repetition to eliminate any potential beam instability caused by non-related transfocator reasons. To define the averaged position of the beam in a single repetition, we measured the center of mass at all 50 images, implementing custom-made Python code and a skimage module (van der Walt *et al.*, 2014). The standard deviation of the center of mass over 50 images was equal to 0.25 μm and 0.07 μm, which corresponds to the random measurement error of 0.5 μm and 0.14 μm in the horizontal and vertical directions, respectively (multiplication by 2 is defined by Student's *t*-distribution (Student, 1908) for $N = 50$ measurements and 95% confidence level).

In the final result [Fig. 3(*c*)], the focal spot deviated within the range of 1.2 μm and 0.7 μm in the horizontal and vertical directions, respectively, indicating that the optical axis of the UCTF deviated by the same value. This number was again calculated with the doubling of the standard deviation of the beam position over 15 repetitions (factor of 2 is defined by Student's *t*-distribution for $N = 15$ measurements and 95% confidence level). The obtained numbers (1.2 μm and 0.7 μm) characterize the overall instrumental error of the transfocator and correspond to the average shift of single lenses in the CRL. They also fully satisfy micro-scale lens positioning requirements (Andrejczuk *et al.*, 2010).

## 4. Conclusions

In the present paper, we designed and manufactured a new UCTF for the first time. The device has minimal gaps between individual X-ray refractive lenses and can be used to change the number of lenses by moving them one-by-one independently. The mechanical performance of the device was successfully tested both in laboratory and synchrotron setups, where the UCTF demonstrated high accuracy in the mechanical positioning of individual lenses. All materials and individual assemblies of the device are vacuum compatible but can also be used in air. In addition, Python-based software can be easily integrated into most modern synchrotron beamline controlling systems. Hence, the device is easy to operate and, in combination with small overall size and light weight, allows one to integrate it at various experimental setups.

In contrast to cartridge-type transfocators, the UCTF provides smooth and linear shifts of focal positions over the entire working range, whereas cartridge-type transfocators change focal length unevenly along the optical axis. This is caused by the fact that the cartridge-type lens arrangement inevitably leaves empty spaces between individual cartridges and these gaps vary in a complicated way when switching from one set of cartridges to another. Therefore, the optical properties of the lens system are affected throughout the entire focal length range. In contrast, the UCTF is based on a single-lens approach, with the minimal distance between individual lenses, which solves the problem of an uncontrolled arrangement of empty spaces between cartridges.

Providing permanent energy and focal length tunability, the UCTF is able to be either a beam collimation system or a short-focal magnifying objective, thus being suitable for a wide range of applications even at non-specialized imaging beamlines. It is particularly important for non-destructive *in situ* or *in vivo* measurements in various areas of X-ray science, where fast tracking of dynamical, morphological and structural changes is critical. The device can be also used for precise measurements of source sizes and emittances at third- and fourth-generation synchrotron X-ray sources (Ewald *et al.*, 2011). Currently, the device is mounted at the second end-station of EMBL P14 beamline, shaping the beam for time-resolved pump–probe serial crystallography experiments.

## Funding information

This research was supported by Russian Science Foundation Project No. 19-72-30009 (experimental tests) and by the Russian Academic Excellence Project at the Immanuel Kant

Baltic Federal University (design and manufacturing of the device).

## References


Andrejczuk, A., Krzywiński, J., Sakurai, Y. & Itou, M. (2010). *J. Synchrotron Rad.* **17**, 616–623.

Baron, A. Q. R., Kohmura, Y., Krishnamurthy, V. V., Shvyd'ko, Y. V. & Ishikawa, T. (1999). *J. Synchrotron Rad.* **6**, 953–956.

Barthelmess, M., Englisch, U., Pflüger, J., Schöps, A., Skupin, J. & Tischer, M. (2008). *Proceedings of the 11th biennial European Particle Accelerator Conference (EPAC08)*, 23–27 June 2008, Genoa, Italy, pp. 2320–2322.

Bosak, A., Snigireva, I., Napolskii, K. S. & Snigirev, A. (2010). *Adv. Mater.* **22**, 3256–3259.

Bowler, M. W., Nurizzo, D., Barrett, R., Beteva, A., Bodin, M., Caserotto, H., Delagenière, S., Dobias, F., Flot, D., Giraud, T., Guichard, N., Guijarro, M., Lentini, M., Leonard, G. A., McSweeney, S., Oskarsson, M., Schmidt, W., Snigirev, A., von Stetten, D., Surr, J., Svensson, O., Theveneau, P. & Mueller-Dieckmann, C. (2015). *J. Synchrotron Rad.* **22**, 1540–1547.

Buffet, A., Rothkirch, A., Döhrmann, R., Körstgens, V., Abul Kashem, M. M., Perlich, J., Herzog, G., Schwartzkopf, M., Gehrke, R., Müller-Buschbaum, P. & Roth, S. V. (2012). *J. Synchrotron Rad.* **19**, 647–653.

Byelov, D. V., Meijer, J. M., Snigireva, I., Snigirev, A., Rossi, L., van den Pol, E., Kuijk, A., Philipse, A., Imhof, A., van Blaaderen, A., Vroege, G. J. & Petukhov, A. V. (2013). *RSC Adv.* **3**, 15670–15677.

Chumakov, A. I., Rüffer, R., Leupold, O., Barla, A., Thiess, H., Asthalter, T., Doyle, B. P., Snigirev, A. & Baron, A. Q. R. (2000). *Appl. Phys. Lett.* **77**, 31–33.

Dimper, R., Reichert, H., Raimondi, P., Sánchez Ortiz, L., Sette, F. & Susini, J. (2014). *ESRF Upgrade Programme Phase II (2015–2022)*, p 190. ESRF, Grenoble, France.

Drakopoulos, M., Snigirev, A., Snigireva, I. & Schilling, J. (2005). *Appl. Phys. Lett.* **86**, 1–4.

Dubrovinskaia, N., Dubrovinsky, L., Solopova, N. A., Abakumov, A., Turner, S., Hanfland, M., Bykova, E., Bykov, M., Prescher, C., Prakapenka, V. B., Petitgirard, S., Chuvashova, I., Gasharova, B., Mathis, Y. L., Ershov, P., Snigireva, I. & Snigirev, A. (2016). *Sci. Adv.* **2**, e1600341.

Ershov, P. A., Kuznetsov, S. M., Snigireva, I. I., Yunkin, V. A., Goikhman, A. Y. & Snigirev, A. A. (2015). *J. Surf. Invest.* **9**, 576–580.

Ewald, F., Elleaume, P., Farvacque, L., Franchi, A., Robinson, D., Scheidt, K., Snigirev, A. & Snigireva, I. (2011). *Proceedings of the 10th European Workshop on Beam Diagnostics and Instrumentation for Particle Accelerators (DIPAC2011)*, 16–18 May, 2011, Hamburg, Germany, pp. 188–190.

Polikarpov, M., Polikarpov, V., Snigireva, I. & Snigirev, A. (2016). *Phys. Proc.* **84**, 213–220.

Polikarpov, M., Snigireva, I. & Snigirev, A. (2014). *J. Synchrotron Rad.* **21**, 484–487.

Polikarpov, M., Snigireva, I. & Snigirev, A. (2016). *AIP Conf. Proc.* **1741**, 040024.

Santoro, G., Buffet, A., Döhrmann, R., Yu, S., Körstgens, V., Müller-Buschbaum, P., Gedde, U., Hedenqvist, M. & Roth, S. V. (2014). *Rev. Sci. Instrum.* **85**, 043901.

Simons, H., King, A., Ludwig, W., Detlefs, C., Pantleon, W., Schmidt, S., Stöhr, F., Snigireva, I., Snigirev, A. & Poulsen, H. F. (2015). *Nat. Commun.* **6**, 1–6.

Snigirev, A., Ershov, P., Snigireva, I., Hanfland, M., Dubrovinskaia, N. & Dubrovinsky, L. (2018). *Microsc. Microanal.* **24**, 238–239.

Snigirev, A., Kohn, V., Snigireva, I. & Lengeler, B. (1996). *Nature*, **384**, 49–51.

Snigirev, A. & Snigireva, I. (2008). *C. R. Phys.* **9**, 507–516.

Snigirev, A., Snigireva, I., Grigoriev, M., Yunkin, V., Di Michiel, M., Kuznetsov, S. & Vaughan, G. (2007). *Proc. SPIE*, **6705**, 670506–670511.

Snigirev, A., Snigireva, I., Kohn, V., Yunkin, V., Kuznetsov, S., Grigoriev, M. B., Roth, T., Vaughan, G. & Detlefs, C. (2009). *Phys. Rev. Lett.* **103**, 064801.

Snigirev, A., Snigireva, I., Lyubomirskiy, M., Kohn, V., Yunkin, V. & Kuznetsov, S. (2014). *Opt. Express*, **22**, 25842–25852.

Snigirev, A., Snigireva, I., Vaughan, G., Wright, J., Rossat, M., Bytchkov, A. & Curfs, C. (2009). *J. Phys. Conf. Ser.* **186**, 012072.

Snigirev, A. A., Yunkin, V., Snigireva, I., Di Michiel, M., Drakopoulos, M., Kouznetsov, S., Shabel'nikov, L., Grigoriev, M., Ralchenko, V., Sychov, I., Hoffmann, M. & Voges, E. I. (2002). *Proc. SPIE*, **4783**, 1–9.

Student (1908). *Biometrika*, **6**, 1–25.

Strempfer, J., Francoual, S., Reuther, D., Shukla, D. K., Skaugen, A., Schulte-Schrepping, H., Kracht, T. & Franz, H. (2013). *J. Synchrotron Rad.* **20**, 541–549.

Vaughan, G. B. M., Wright, J. P., Bytchkov, A., Rossat, M., Gleyzolle, H., Snigireva, I. & Snigirev, A. (2011). *J. Synchrotron Rad.* **18**, 125–133.

Walt, S. van der, Schönberger, J. L., Nunez-Iglesias, J., Boulogne, F., Warner, J. D., Yager, N., Gouillart, E. & Yu, T. (2014). *PeerJ.* **2**, e453.

Zozulya, A. V., Bondarenko, S., Schavkan, A., Westermeier, F., Grübel, G. & Sprung, M. (2012). *Opt. Express*, **20**, 18967–18976.

Zverev, D., Barannikov, A., Snigireva, I. & Snigirev, A. (2017). *Opt. Express*, **25**, 28469.

Zverev, D., Snigireva, I., Kohn, V., Kuznetsov, S., Yunkin, V. & Snigirev, A. (2018). *Microsc. Microanal.* **24**, 162–163.